



LAWRENCE  
LIVERMORE  
NATIONAL  
LABORATORY

# Deformation Behavior of Nanoporous Metals

J. Biener, A. M. Hodge, A. V. Hamza

November 29, 2007

Micro and Nano Mechanical Testing of Materials and Devices

## **Disclaimer**

---

This document was prepared as an account of work sponsored by an agency of the United States government. Neither the United States government nor Lawrence Livermore National Security, LLC, nor any of their employees makes any warranty, expressed or implied, or assumes any legal liability or responsibility for the accuracy, completeness, or usefulness of any information, apparatus, product, or process disclosed, or represents that its use would not infringe privately owned rights. Reference herein to any specific commercial product, process, or service by trade name, trademark, manufacturer, or otherwise does not necessarily constitute or imply its endorsement, recommendation, or favoring by the United States government or Lawrence Livermore National Security, LLC. The views and opinions of authors expressed herein do not necessarily state or reflect those of the United States government or Lawrence Livermore National Security, LLC, and shall not be used for advertising or product endorsement purposes.

# 1 Deformation behavior of nanoporous metals

Juergen Biener<sup>1</sup>, Andrea M. Hodge<sup>2</sup>, Alex V. Hamza<sup>1</sup>

<sup>1</sup>Nanoscale Synthesis and Characterization Laboratory, Lawrence Livermore National Laboratory, Livermore, California 94550, USA

<sup>2</sup>Aerospace and Mechanical Engineering Department, University of Southern California, Los Angeles, CA 90089

## 1.1 Introduction

Nanoporous open-cell foams are a rapidly growing class of high-porosity materials (porosity  $\geq 70\%$ ). The research in this field is driven by the desire to create functional materials with unique physical, chemical and mechanical properties where the material properties emerge from both morphology and the material itself. An example is the development of nanoporous metallic materials for photonic and plasmonic applications which has recently attracted much interest. The general strategy is to take advantage of various size effects to introduce novel properties. These size effects arise from confinement of the material by pores and ligaments, and can range from electromagnetic resonances [1] to length scale effects in plasticity.[2, 3]

In this chapter we will focus on the mechanical properties of low density nanoporous metals and how these properties are affected by length scale effects and bonding characteristics. A thorough understanding of the mechanical behavior will open the door to further improve and fine-tune the mechanical properties of these sometimes very delicate materials, and

thus will be crucial for integrating nanoporous metals into products. Cellular solids with pore sizes above 1 micron have been the subject of intense research for many years, and various scaling relations describing the mechanical properties have been developed.[4] In general, it has been found that the most important parameter in controlling their mechanical properties is the relative density, that is, the density of the foam divided by that of solid from which the foam is made. Other factors include the mechanical properties of the solid material and the foam morphology such as ligament shape and connectivity. The characteristic internal length scale of the structure as determined by pores and ligaments, on the other hand, usually has only little effect on the mechanical properties. This changes at the submicron length scale where the surface-to-volume ratio becomes large and the effect of free surfaces can no longer be neglected. As the material becomes more and more constraint by the presence of free surfaces, length scale effects on plasticity become more and more important and bulk properties can no longer be used to describe the material properties. Even the elastic properties may be affected as the reduced coordination of surface atoms and the concomitant redistribution of electrons may soften or stiffen the material. If, and to what extent, such length scale effects control the mechanical behavior of nanoporous materials depends strongly on the material and the characteristic length scale associated with its plastic deformation. For example, ductile materials such as metals which deform via dislocation-mediated processes can be expected to exhibit pronounced length scale effects in the sub-micron regime where free surfaces start to constrain efficient dislocation multiplication. In this chapter we will limit our discussion to our own area of expertise which is the mechanical behavior of nanoporous open-cell gold foams as a typical example of nanoporous metal foams. Throughout this chapter we will review our current understanding of the mechanical properties of nanoporous open-cell foams including both experimental and theoretical studies.

## 1.2 Processing Techniques

Nanoporous metal foams have been made in various shapes such as nanowires,[5, 6] thin-films,[7, 8] and macroscopic 3D samples.[8, 9] Their morphology ranges from disordered three-dimensional network structures (sponge-like morphology) to well-defined periodic thin-film structures with excellent long-range order which are mostly used for photonic applications. This section provides a short review of the synthesis of non-periodic nanoporous metal foams which can be prepared in the form of

very uniform millimeter-sized 3D objects. A typical example of the sponge-like open-cell foam morphology of np-Au is shown in Figure 1a.

Synthesis techniques include top-down (dealloying) and bottom-up strategies (filter casting and templating) as well as combinations thereof. Many of these techniques have been developed or further refined at Lawrence Livermore National Laboratory with the ultimate goal to design a new class of three-dimensional nanoporous metals for high energy density laser experiments. This application requires the fabrication of millimeter-sized, defect-free monolithic samples of nanoporous materials with well-defined pore-size distributions (including hierarchical porosities) and adjustable densities down to a few atomic percent. Yet the material has to be mechanically robust enough to be machined. An example of such a Laser target is shown in Figure 1b.

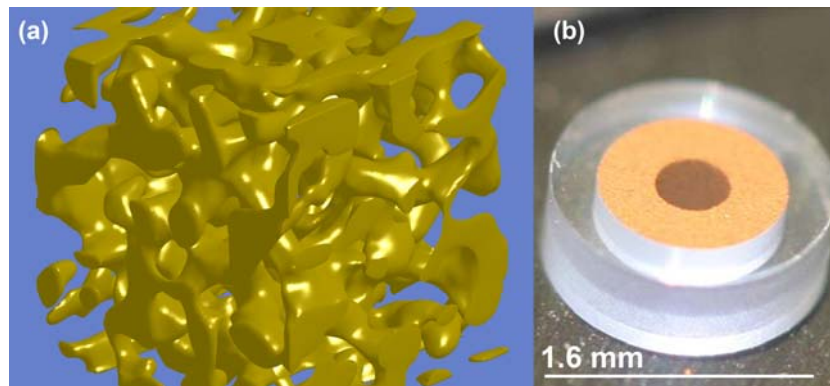


**Fig. 1.** (a) Focused ion beam nanotomography (FIB-nt) image showing the 3D-structure of nanoporous Au. This state-of-the-art FIB-nt image was collected by L. Holzer, Ph. Gasser and B. Münch from EMPA, Switzerland. The resolution of  $2 \times 3 \times 6$  nm presents the current record of the FIB-nt method, and allows one to determine microstructural parameters responsible for mechanical size effects of nanoporous materials. (b) Machined ultra-low density Au foam target for high-energy-density Laser experiments. The picture was provided by courtesy of Craig Akaba, LLNL

### 1.2.1. Dealloying

Dealloying is by far the most often applied method to generate macroscopic 3D as well as 2D (thin-film) and 1D (nanowire) samples of low-

density nanoporous metal foams for nanomechanical testing. In metallurgy, dealloying is defined as selective corrosion (removal) of the less noble constituent from an alloy, usually via dissolving this component in a corrosive environment.[10, 11] In case of binary solid-solution alloys with a narrow compositional range around  $A_{0.7}B_{0.3}$  (where B is the less noble alloy constituent) this process can lead to spontaneous pattern formation, that is, development of a three-dimensional bicontinuous nanoporous structure while maintaining the original shape of the alloy sample. The material can be very uniform, even on a macroscopic length scale, and typically exhibits a specific surface area in the order of a few  $m^2/g$ . [12] The best-studied example is the formation of nanoporous gold (np-Au) via selective removal of Ag from a AuAg alloy,[7, 8, 11] but other alloys such as AuAl<sub>2</sub>, [13] MnCu (np-Cu), [14] and CuPt (np-Pt) [15] have also been successfully dealloyed. The process can be easily extended to two-dimensional thin-film samples by using commercially available white-gold leaves with a thickness of a few hundred nanometers [7] or thin sputter-deposited alloy films. [16, 17] Even one-dimensional structures such as nanoporous Au nanowires can be fabricated by using combination of electrochemical templating and dealloying. [5] The characteristic sponge-like open-cell foam morphology of np-Au is illustrated by the focused ion beam nanotomography image shown in Figure 1a.

Nanoporous Au is ideally suited to study length scale effects in nanoporous metal foams due to its unique annealing behavior: The length scale of both pores and ligaments can easily be adjusted by a simple thermal treatment in ambient over a wide range from 3 nm to the micron length scale. [18-20] Most notably, the material rearrangement during annealing does not affect the relative density or relative geometry of the material (ligament connectivity or ligament, pore, and sample shape). [18, 21] An example of such an annealing experiment is shown in Figure 2.

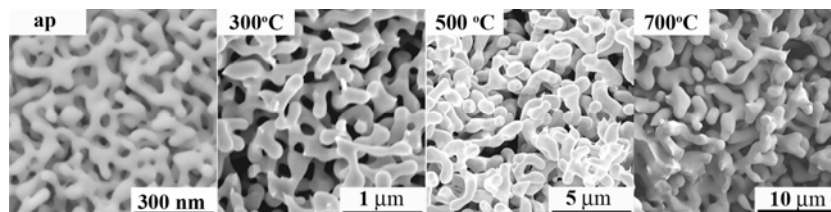


**Fig. 2.** Cross-sectional SEM micrographs of as-prepared (ap) and annealed np Au: 300 °C, 500 °C, 700 °C. Note the self-similarity of the structure while increasing the feature size by more than a factor of 30. The relative density of the materials remains constant at approximately 30%

The dealloying technique can also be used to introduce even more complicated morphologies such as hierarchical porosities. For example, bimodal pore size distributions can be realized by using a 3-step dealloying/annealing/dealloying strategy where a micron-scale ligament structure is first generated by dealloying followed by annealing, and nano-scale porosity is finally reintroduced into the ligaments by a second dealloying step. This approach requires either the use of a ternary alloys as starting material, or relies on metal deposition after the first dealloying/annealing step.[22] For example, we have used ternary Cu-Ag-Au alloys to prepare low-density ( $\sim 10$  at.% relative density) nanoporous Au samples with a bimodal pore size distribution. However, preparation of the appropriate homogeneous single phase ternary alloy is challenging and limits the applicability of this approach.

### 1.2.2. Bottom-up approaches

Although the bottom-up approach to nanostructured metal foams is very versatile regarding the range of accessible densities and morphologies, very little is known about the mechanical properties of the resulting materials. The technique usually involves the use of sacrificial organic materials such as polystyrene (PS) micro beads as templates to generate a nanostructured porous solid.[23, 24] The dimensions of the template directly determine the length scale of the porosity in the final structure. The technique also provides a powerful approach to create materials with complex hierarchical porosities, specifically in combination with dealloying.

In the case of Au foams, the synthesis starts with the preparation large quantities of Au or Ag-Au coated core-shell particles. These man-made building blocks are then assembled (casted) into a monolithic porous structure using a procedure analogous to the slip-casting process of ceramic [25] and metal [24] particles. Finally, the pure Au foam sample is obtained by removing the PS template by a simple heat treatment (Figure 3). If Ag-Au coated core-shell particles were used as a starting material one easily can introduce hierarchical porosities by adding a dealloying step. The technique out-lined above has been successfully used to fabricate millimeter-sized, defect-free monolithic samples of nanoporous Au with well-defined pore-size distributions and densities down to a few atomic percent (see for example the Laser target shown in Figure 1b).

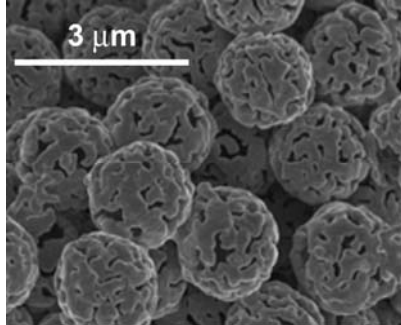


**Fig. 3.** Ultra-low density metal foam (1g/cc) prepared from hollow 1 micron diameter  $\text{Ag}_{0.7}\text{Au}_{0.3}$  shells. The SEM micrograph was provided by courtesy of G.W. Nyce, LLNL

### 1.3. Deformation Behavior

#### 1.3.1 Macroporous foams

Before going into further details on the deformation behavior of nanoporous foams, it is beneficial to cover the basics of foam mechanics. To keep this discussion short, we will only address the deformation behavior of open-cell foams. A complete discussion can be found in “Cellular Solids” by Gibson and Ashby.[4]

Our knowledge on foam mechanics comes almost exclusively from the study of macroporous foams with cell sizes exceeding one micron. As stated in the introduction, the behavior of such materials is governed by the properties of the base material and the porosity, or more specifically, the relative density ( $\rho^*/\rho_s$ ) which is defined as the density of the foam ( $\rho^*$ ) divided by the density of the material it is made of ( $\rho_s$ ). A variety of scaling relations has been developed to predict and describe the properties of cellular solids using these two parameters. For example, by compiling experimental data collected from a wide variety of open-cell foams it can be shown that the yield strength ( $\sigma$ ) and the Young’s modulus ( $E$ ) of open-cell foams can be described by the following scaling relations:

$$\sigma^* = C_2 \sigma_s \left( \frac{\rho^*}{\rho_s} \right)^{3/2} \quad (1)$$

$$E^* = C_1 E_s \left( \frac{\rho^*}{\rho_s} \right)^2 \quad (2)$$

where \* refers to foam properties and  $s$  to the bulk properties, and  $C_1=1$  and  $C_2=0.3$  are fitting constants. It is important to notice that these scaling relations contain no explicit length scale dependence and assume that the material properties of the ligaments such as the yield strength and the Young's modulus are size-independent and equal to the bulk value. As will be discussed below, this assumption is no longer valid for metallic foams with submicron features.

Experimentally, the mechanical behavior of foams is typically studied in compression; however, tensile testing has been used as well.[26, 27] In the case of a uniaxial compression test the typical stress –strain deformation curve for an elastic-plastic foam will be composed of a linear elastic regime followed by a collapse plateau followed by a densification regime (Fig. 4).

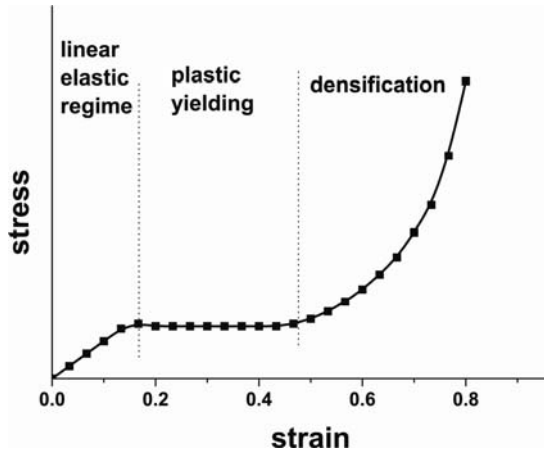


**Fig. 4.** Representative compressive stress-strain behavior of a metal foam showing regimes of elastic and plastic deformation until densifications dominates

Indentation is another frequently used technique to assess hardness and yield strength data of cellular solids.[28-32] In the case of low-density foams ( $\rho^*/\rho_s \leq 0.3$ ), it is generally assumed that the indentation hardness ( $H$ ) is approximately equal to the yield strength,  $H \sim \sigma_y$ , rather than following the  $H \sim 3\sigma_y$  relationship typically observed for fully dense materials.[4] The reason for this is that the material under the indenter is not constrained by the surrounding material as it densifies with very little lateral spread (which translates into an effective Poisson's ratio  $\sim 0$ ). The  $H \sim \sigma_y$  relationship has been validated by a number of studies, and is used throughout this review to assess the yield strength of low-density metal foams from nanoindentation hardness data. However, it has to be pointed out that this relationship is only valid for foams with at least 60% porosity and when issues such as indentation size effects and densification are properly accounted for. A detailed discussion on this topic can be found in a recent publication.[21]

### 1.3.2 Nanoporous Foams

In the case of nanoporous materials, the majority of studies have relied on nanoindentation as a tool to measure mechanical properties such as yield strength and Young's modulus.[33-35] The technique has the advantage of being experimentally simple and, compared to other techniques, of having relatively low requirements regarding sample size or defect concentration. Furthermore, nanoindentation can be easily applied to thin-films and irregularly shaped samples as long as the surface roughness is low. Other, experimentally more complex methods are pillar micro-compression tests [36, 37] and film or beam bending tests.[16, 35, 38, 39] Examples of nanoindentation and beam deflection tests are shown in Figure 5. In the case of nanoindentation, the yield strength is typically obtained by assuming that  $\sigma_y \sim H$  as discussed above. Given that more studies have addressed the yield strength, we will start with a discussion of the yield strength data, followed by a short review on the elastic properties of nanoporous Au.

#### ***Strength and modulus***

Nanoporous Au has been the preferred material in the majority of studies in this field.[21, 33-36, 40] As outlined above, the material is ideally suited to study length scale effects on plasticity in nanoporous metal foams as the pore size is experimentally simple to control, for example by annealing. Another material systems studied is nanoporous Cu.[14] The two most often reported properties are yield strength and elastic modulus, and the

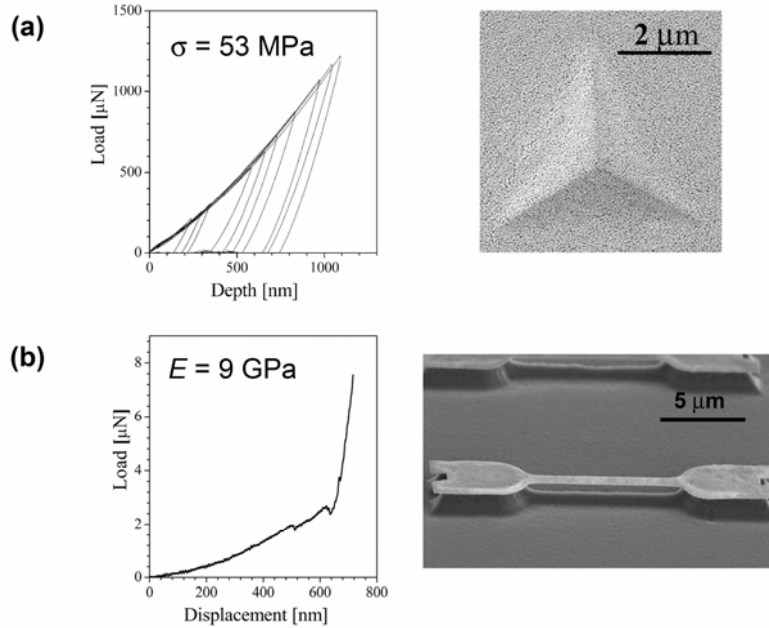


**Fig. 5.** Typical examples of nanomechanical tests performed on nanoporous Au: (a) Series of nanoindentation load-displacement curves using a Berkovich tip (left) and a SEM micrograph showing a typical residual impression of such a test (right). This specific test was performed on nanoporous Au with a relative density of 0.25 and an average ligament width of 30 nm, and reveals a yield strength of 53 MPa. (b) Load-displacement curve of a deflective tensile test performed on micro-fabricated dog-bone samples (left). Curve fitting to non-linear beam theory reveals an elastic modulus of  $\sim 9 \text{ GPa}$  (relative density  $\sim 0.35$ , ligament width 20-40 nm). SEM micrograph of a dog-bone sample for deflective tensile tests (right). The tensile test data were provided by courtesy of J.W. Kysar, Columbia University (New York)

reported values for these properties range from 15 MPa to 240 MPa and 7 GPa to 40 GPa, respectively (Figure 6). Surprisingly, and despite its high porosity, nanoporous Au (240 MPa) can be stronger than bulk Au (200 MPa for severely worked single Au crystals). It is instructive to compare these values with the predictions made by the Gibson and Ashby scaling relations. One can calculate the yield strength and the Young's modulus of nanoporous Au as a function of relative density using Eqs. 1 and 2, and the bulk properties of Au as input. The yield strength of bulk Au is very dependent on the sample history, and values as low as 2 MPa for well-

annealed and as high as  $\sim 200$  MPa for severely worked single crystals have been reported (see for example Ref. [41] and references therein). To be conservative, we will use the high-end value of  $\sim 200$  MPa, and the average value of the elastic modulus,  $\sim 80$  GPa.[42] Assuming that the relative densities range from 25 to 42%, Eqs. 1 and 2 then predict yield strength values from 7.5 to 16 MPa and elastic modulus values from 5 to 14 GPa (see solid lines in Figure 6). Clearly, the experimental data do not follow the prediction made by the scaling relations: Specifically the yield strength data are higher than predicted, sometimes by more than an order of magnitude. The Young's modulus seems to be better described by the scaling equations, but the data are still very scattered. Furthermore, one can observe length scale effects not predicted by the Gibson and Ashby scaling relations. For example, the yield strength of nanoporous Au with relative density of 30% increases from  $\sim 10$  MPa to  $\sim 100$  MPa as the ligament sizes decreases from 900 nm to 40 nm.[21] In conclusion, only for the largest ligaments a reasonable agreement between experiment and theory is observed.

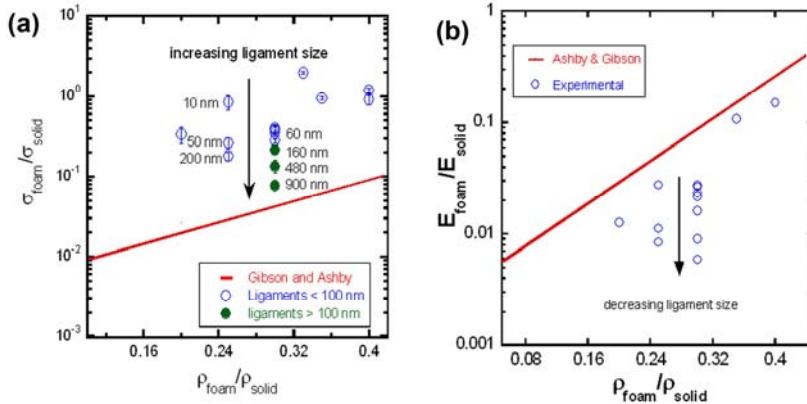


**Fig. 6.** Calculated (lines) and experimental (symbols) yield strength (a) and Young's modulus (b) data of nanoporous Au plotted as a function of the relative density of the material. Both yield strength and Young's modulus have been normalized using  $\sigma_{\text{solid}} = 200$  MPa and  $E_{\text{solid}} = 80$  GPa as the yield strength and Young's modulus of fully dense Au

To compile data obtained from samples with different relative densities and check for length scale effects, it is instructive to use equation 1 and 2 to calculate the mechanical properties of the ligament material, and plot the result as a function of the ligaments size. The result of such a data compilation is shown in Figure 7. Figure 7a reveals that the calculated strength of the ligament materials increases with decreasing feature size, independent

of the testing method. This is in contrast to previous studies on macro-cellular foams which found that for a given porosity the cell size had a minimal effect in the mechanical behavior.[43, 44] Clearly, this is not true for the nanoporous foams. In contrast, as revealed by Figure 7a, the majority of studies on nanoporous Au observe that the yield strength of the ligaments in nanoporous Au approaches the theoretical shear stress  $G/2\pi$  of Au ( $\sim 4.3$  GPa) as the ligament size decreases to the 10 nm length scale.

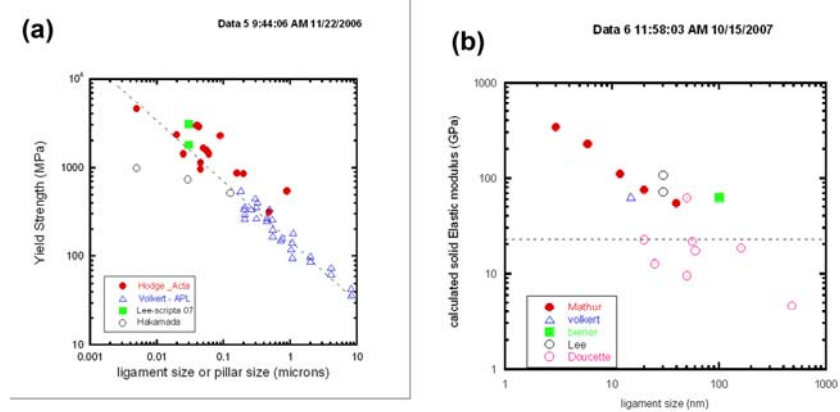


**Fig. 7.** Calculated ligament yield strength (*a*) and modulus (*b*) as a function of ligament diameter. Also included are data obtained by microcompression test on Au pillars

The high yield strength of the ligaments of np-Au is consistent with recent nanomechanical measurements performed on submicron Au columns [41, 45, 46] and nanowires.[47] Both of these test specimens closely resemble the ligaments in foams, and mechanical tests reveal the general trend that “smaller is stronger”. For example, Geer and Nix [45, 46] reported that the yield strength of submicron Au columns fabricated by focused ion beam micromachining approaches the theoretical yield strength of Au as the column diameter decreases to a few hundred nanometer. Specifically the yield strength data reported by Volkert and Lilleodden [41] are in excellent agreement with the size dependence observed for nanoporous Au: the yield strength of submicron Au columns follows the power law  $d^n$ , where  $d$  is the column diameter and  $n$  is 0.6. Figure 7a suggests that this size dependence continues to be valid down to 10 nm, the smallest ligament size which has been tested so far.

The size dependence of the yield strength observed in column micro-compression tests has been explained by “dislocation starvation”, that is

the absence of efficient, easy-to-activate dislocation sources in sub-micron samples due to the presence of free surfaces. The argument goes along the following line: The smaller the sample volume (column/ligament), the smaller the dislocation source which can still be accommodated, the higher the stresses which are required to initiate yield. In this context, np Au can be envisioned as a three-dimensional network of defect-free, ultra-high strength Au nanowires.[37] Length-scale effects in plasticity can also be studied theoretically using molecular dynamics (MD) simulations.[48, 49] Preliminary molecular dynamics (MD) results show indeed that it is difficult to incorporate stable dislocation sources (such as a Frank-Read source) in nm-sized ligaments. These simulations also reveal that plastic deformation of nm-sized Au columns is still dislocation-mediated, and that these dislocations nucleate in the vicinity of step edges on free surfaces at stress levels close to the theoretical strength of the material (Figure 8).[49] Dislocation-mediated plasticity of nanometer-sized ligaments in nanoporous Au has recently also been observed experimentally using an in-situ transmission electron microscope nanoindentation technique.[50]

Additional factors which potentially could contribute to the higher-than-predicted strength are: testing method, densification, and grain size. For example, nanoindentation hardness and strength data obtained from fully dense materials show frequently higher values than those obtained by macroscopic tests, which is commonly attributed to the so-called “indentation size effect”. We discard this possibility as the strength of nanoporous Au has been tested by a variety of different testing methods and generally good agreement has been found. Specifically, the micro-compression tests on nanoporous Au performed by Volkert et al.[36] have shown that the measured strength is independent of the test volume, consistent with the idea that the size effects in nanoporous Au are dominated by the ligament/pore dimensions and not by the sample size. Similarly, densification effects can be ruled out as the increase of strength with decreasing ligament size was observed for a fixed initial foam density. Finally, the grain structure of the ligaments or the lack thereof is still a subject of debate and is beyond the scope of this discussion [9]. However, even if we assume that the ligaments develop a nanocrystalline grain structure during dealloying, this would still not account for the high strength found experimentally since the yield strength of nanocrystalline Au [51, 52] is only 4 times higher than that of coarse-grained material.

The elastic properties of nanoporous Au have attracted less interest, and consequently there are fewer data available which, in addition, appear

to be more scattered (Fig. 6b and Fig.7b). Most studies report Young's modulus values in the 5 to 13 GPa range consistent with the predictions

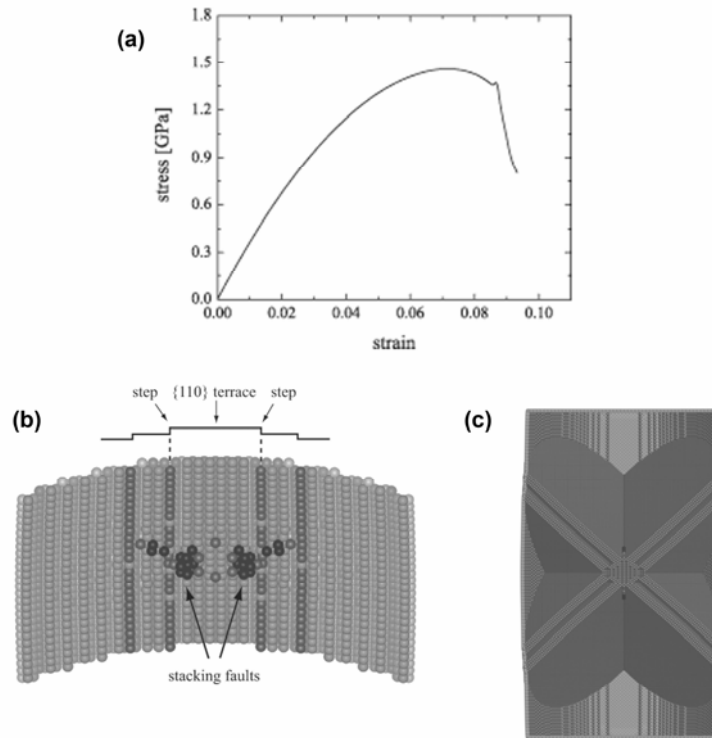


**Fig. 8.** Mechanical response of nanoscale Au pillars under compressive loading studied by MD. The displayed data were obtained from a 20 nm by 40 nm Au pillar compressed at 0K: a) Compressive stress-strain curve demonstrating the high yield strength of nanoscale Au ligaments; b) Nucleation of partial dislocations near the step edges revealing dislocation-mediated plasticity; c) Final state after 10% compression. The MD results were provided by courtesy of Dr. L. A. Zepeda-Ruiz and Dr. B. Sadigh, LLNL

made by Eqn. 2 if one uses the bulk modulus of Au ( $\sim 80$  GPa) and relative densities ranging from 0.25 to 0.4. An exception to this is the recent study by Mathur and Erlenbacher [40] who reported a 4-fold increase in the Young's modulus, from  $\sim 10$  GPa to  $\sim 40$  GPa, as the ligament diameter decreases from  $>12$  nm to 3 nm. The narrow range of most of the available data seems to indicate that there are little or no size effects in the elastic

properties. In principle, the high surface-to-volume ratio of the nanoscale ligaments in nanoporous Au could give rise to a size effect in the elastic properties: One can think of the ligaments as core-shell structures, where the core has bulk-like properties, and the shell exhibits elastic properties reflecting the reduced coordination number of surface atoms.[53] Depending on the actual electron redistribution caused by reduced coordination, the surface can become either softer or stiffer. Recent theoretical studies on Cu [54] showed that the effect of free surfaces on elasticity depends also on crystal orientation. However, even in the extreme case of a 2-layer system, the Young's modulus did not change by more than 50%.

Mathur and Erlenbacher [40] attributed the increased stiffness of ultra-fine nanoporous Au to a combination of surface stress, density increase during dealloying due to shrinkage, and a higher bending stiffness of smaller ligaments. However, the 'smaller-is-stiffer' trend could also be caused by an increased level of residual Ag in sub-10-nm material. The preparation of this ultra-fine material requires dealloying conditions which strongly suppress surface diffusion. Experimentally, this can be achieved by using either dealloying potentials close to the Au oxidation potential,[55] or by performing the dealloying process at low temperatures.[20] Both methods have been shown to increase the amount of residual Ag which affects both the relative density and the elastic properties of the material. Unfortunately, many studies do not report the residual silver content, thus making the comparison from study to study more difficult. The effect of residual Ag on the elastic properties of nanoporous Au has recently been studied by Doucette et al.[56], who found that Ag doping generally increases the Young's modulus of nanoporous Au.

As mentioned above, one can think of nanoporous Au as a 3D network of Au nanowires. Thus it is instructive to compare the data discussed above with the literature on Au nanowires. Wu et al.[47] studied mechanical properties of Au nanowires ranging from 40 nm to 250 nm in diameter, and reported a Young's modulus of ~70 GPa, independent of the nanowire diameter and close to the value of bulk gold. Similar observations, namely a bulk-like behavior, have been reported for submicron Au columns.[41] The mechanical properties of sub-10-nm Au nanowires and pillars have been the subject of several molecular dynamics studies. Generally it was observed that the Young's modulus is only weakly dependent on the wire/pillar diameter (for wires which do not undergo a phase transformation [53]), and close to the value of bulk gold.[48, 57] Furthermore, it has been shown that the surface stress in these ultra-high surface-to-volume ratio systems mainly affects the strength by creating a compressive stress

state in the wire/pillar core. In conclusion, most data presently available do not support the idea of a pronounced size effect in the elastic properties of nanoporous Au.

### ***Fracture behavior***

As discussed above, nanoporous Au has unique mechanical properties under compressive loading conditions where it combines high strength with high porosity. On the other hand, the material is notoriously brittle which severely limits its usefulness in terms of applications.[18, 58] Actually, the brittleness of nanoporous Au is the reason why scientists started to study the mechanical behavior of nanoporous Au in the first place: Ag-Au alloys were used to study stress corrosion cracking, that is, brittle failure of otherwise ductile materials in a corrosive environment.[59-61] These studies demonstrated that the formation of a thin surface layer of nanoporous gold is responsible for crack initiation and brittle failure of the uncorroded portion of the sample. Given the fact that Au is the most malleable metal, this brittle behavior is surprising. The questions which immediately arise in this context are: What causes the macroscopic brittleness of np-Au? Is the normal dislocation-mediated plasticity suppressed in nanoscale Au ligaments, or is the brittleness simply a consequence of the macroscopic morphology? These are the questions which will be addressed in the following.

The brittleness generally seems to increase with increasing Ag content of the Ag-Au master alloy, at least if dealloying is performed under free corrosion conditions: For example, samples made from  $\text{Ag}_{70}\text{Au}_{30}$  alloys tend to be fairly robust, whereas samples made from  $\text{Ag}_{80}\text{Au}_{20}$  alloys are generally more fragile. This trend seems to correlate with shrinkage and the buildup of tensile stress during dealloying which can induce crack formation.[8] In this context, it is interesting to note that thin-films and nanowires can accommodate this tensile stress better than macroscopic 3D samples as they are less constrained with regard to shrinkage: For example, nanoporous Au nanowires have been successfully prepared from  $\text{Ag}_{82}\text{Au}_{18}$  alloys,[5] whereas a 3D sample prepared from such Ag-rich alloys would typically disintegrate during dealloying due to extensive cracking. The key to crack free material is to avoid dealloying conditions which lead to extensive buildup of tensile stress. Indeed, fracture-resistant nanoporous Au can be prepared by using dealloying conditions which promote stress relaxation, i.e. at elevated temperatures and lower dealloying potentials.[55]

As described above, brittle failure of nanoporous Au is observed under tensile loading conditions. Microstructural characterization of the fracture surfaces reveals that nanoporous Au fails by a combination of intra- and

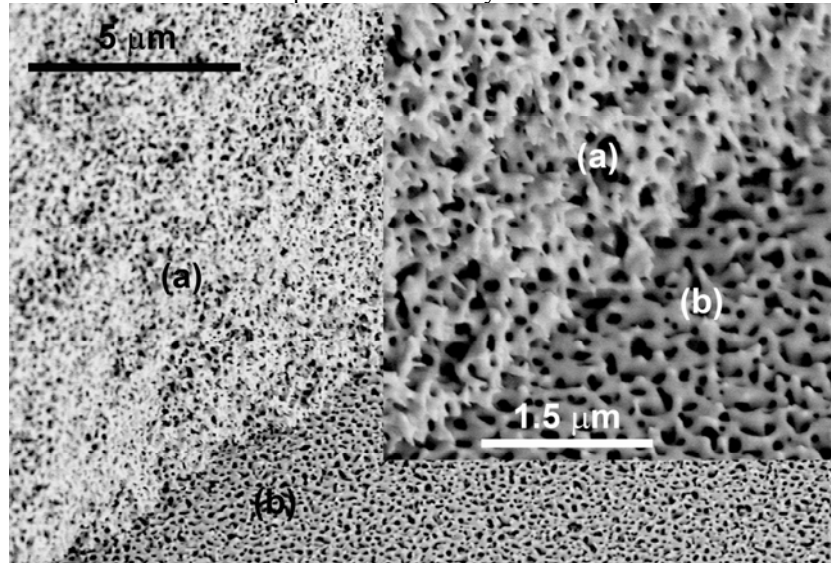


**Fig. 9.** Fracture appearance of nanoporous Au of both intragranular (a) and intergranular regions (b). The inset shows the same region at higher magnification, and reveals the ductile nature of the fracture

intergranular fracture modes [58]: Intergranular fracture, where the crack follows the grain structure of the original AgAu master alloy, reveals itself by the characteristic Rock candy morphology of the fracture surface, whereas intragranular fracture gives rise to smooth and featureless regions. On a microscopic level, however, characteristic necking features reveal ductile failure due to overloading of individual ligaments. In particular regions of intragranular fracture exhibit a high density of disrupted ligaments (Fig. 9). Intergranular fracture surfaces, on the other hand, exhibit a very smooth morphology with only a few disrupted ligaments. This difference can be explained by the presence of extended two-dimensional void-like defects which can be observed along the original grain boundaries of the master alloy. The formation of these defects can be explained by Ag enrichment at the grain boundaries which leads to the development of a reduced density material during dealloying. Indeed, Ag surface segregation during annealing has been reported for the Ag–Au system.[62] The fracture mode described here – brittle on a macroscopic length scale, but microscopically ductile – is not a unique feature of nanoporous gold, but has

recently even been observed for glass which is the common example for brittle failure.[63]

The two-dimensional void-like defects described in the previous paragraph presumably act as crack nucleation sites due to local stress enhancement (Fig 10). Ligaments connecting the regions on opposite sides of a defect experience the highest stress fields and are the first to fail. Once an unstable crack is formed, the crack propagates along the 2D defects until intersecting with another 2D defect at an oblique angle, where the fracture may or may not switch from intergranular to intragranular (see Fig. 9).

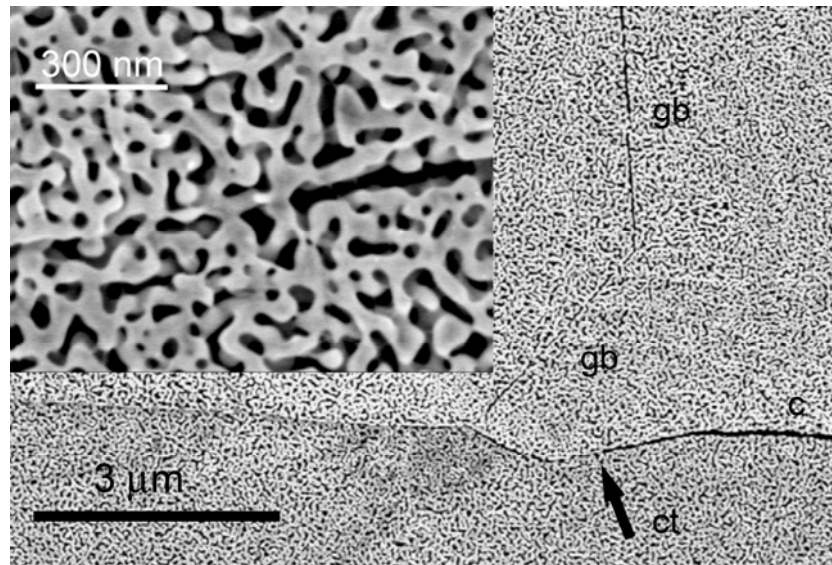


**Fig. 10.** Crack propagation along 2D defects, which are formed during dealloying along the grain boundaries of the original AuAg alloy. The crack (c) propagates from the right to the left along a defect. The remnant of a second grain boundary (gb) can be seen in the upper right. Inset: A higher magnification image of the crack tip (ct) region reveals the void-like character of the 2D defects.

The microscopic ductility of nanoporous Au is particularly obvious in the vicinity of crack tips, where highly strained ligaments still bridging the crack can be found (Fig 11). These ligaments show pronounced necking, and their elongation suggests strain values exceeding 100%. This microscopic ductility is also observed in molecular dynamics simulations on defect-free nanoscale Au columns under tensile loading (Fig 11). Here, the elongation to failure is in the order of 100%, consistent with the finding of

highly strained ligaments near crack tips. The microscopic ductility is a remarkable result in the context of the macroscopic brittleness of np-Au, but is consistent with the fact that Au is the most malleable metal. This immediately raises the question of what causes the macroscopic brittleness of np-Au. A qualitative answer can be found by applying a random fuse network model [64, 65]: According to this model “brittle” failure can be expected for a sufficiently narrow ligament-strength distribution, regardless if the ligaments fail microscopically in a ductile or in a brittle manner. In the limit of a narrow ligament-strength distribution, rupture of the weakest ligament initiates the catastrophic failure of the network structure by overloading adjacent ligaments. The unstable crack then propagates quickly through the bulk of the material following the path of least resistance. This explanation is consistent with the narrow pore size/ ligament width distribution of np-Au observed experimentally, which implies uniform failure strength. The overall strength of a randomly fused network is determined by the largest “critical” defect; that is, the defect that causes the highest stress enhancement at its edge. In the case of nanoporous Au, the two-dimensional void-like defects formed during dealloying along the grain boundaries of the AgAu master alloy serve as crack nucleation sites by concentrating the stress on adjacent ligaments. Thus, instead of plastic deformation of the whole sample, the failure of a few ligaments triggers the brittle fracture of the network. This conclusion may be used to improve the mechanical properties of nanoporous Au by introducing a broader ligament strength distribution and by reducing the number and size of defects.

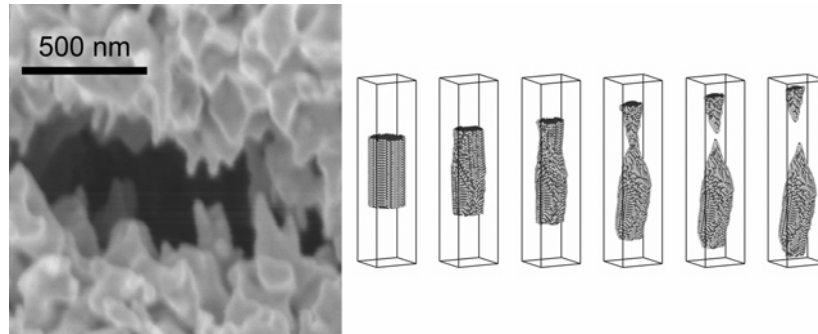


**Fig. 11.** Both SEM micrographs (left) and MD simulations (right) reveal the ductile failure behavior of nanoscale Au ligaments under tensile loading. The Au pillar used in the simulation is 5 nm by 10 nm, and snapshots of the configuration were taken at 0%, 25%, 50%, 100%, 125% and 150% strain. The MD results were provided by courtesy of L.A. Zepeda-Ruiz, LLNL

## 1.4. Summary

In this chapter we have reviewed the mechanical behavior for nanoporous Au. In contrast to macroporous foams, the yield strength of nanoporous Au increases dramatically with decreasing feature size. Consequently, a nanoporous metal foam can be envisioned as a three-dimensional network of ultrahigh-strength nanowires, thus bringing together two seemingly conflicting properties: high strength and high porosity. This highly unusual combination of material properties opens a new door for engineering applications. The elastic properties, on the other hand, seem to be much less affected by the nanoscale morphology of the material and can be reasonably well described by the scaling relations derived from macroporous foams. Currently, the macroscopic brittleness of np-Au presents a major obstacle to applications. This brittleness seems to arise from the network structure rather than reflecting a microscopic brittleness, and thus could potentially be overcome, for example by introducing a broader ligament strength distribution and by eliminating two-dimensional defects. As progress is achieved in understanding the mechanics of nanoporous materials, further research must include different types of nanoporous metals in order to develop more general trends.

## Acknowledgements

This work performed under the auspices of the U.S. Department of Energy by Lawrence Livermore National Laboratory under Contract DE-AC52-07NA27344. The authors would like to acknowledge Beat Muench, Philippe Gasser, Lorenz Holzer, Greg Nyce, Jeffrey Kysar, Luis Zepeda-Ruiz, and Babak Sadigh for providing original figures.

## References

1. Maier SA (2007) *Plasmonics: Fundamentals and Applications*. Springer, New York
2. Arzt E (1998) Size Effects in Materials Due to Microstructural and Dimensional Constraints: A Comparative Review. *Acta Mater* 46: 5611-5626
3. Sieradzki K, Rinaldi A, Friesen C, Peralta P (2006) Length Scales in Crystal Plasticity. *Acta Mater* 54: 4533-4538
4. Gibson LJ, Ashby MF (1997) *Cellular Solids: Structure and Properties*. Cambridge University Press, Cambridge, UK
5. Liu Z, Searson PC (2006) Single Nanoporous Gold Nanowire Sensors. *J Phys Chem B* 110: 4318-4322

6. Yoo SH, Park S (2007) Platinum-Coated, Nanoporous Gold Nanorod Arrays: Synthesis and Characterization. *Adv Mater* 19: 1612-1615
7. Ding Y, Kim YJ, Erlebacher J (2004) Nanoporous Gold Leaf: "Ancient Technology"/Advanced Material. *Adv Mater* 16: 1897-1900
8. Parida S, Kramer D, Volkert CA, Rosner H, Erlebacher J, Weissmuller J (2006) Volume Change During the Formation of Nanoporous Gold by Dealloying. *Phys Rev Lett* 97: 035504
9. Hodge AM, Hayes JR, Caro JA, Biener J, Hamza AV (2006) Characterization and Mechanical Behavior of Nanoporous Gold. *Adv Eng Mater* 8: 853-857
10. Newman RC, Corcoran SG, Erlebacher J, Aziz MJ, Sieradzki K (1999) Alloy Corrosion. *MRS Bulletin* 24: 24-28
11. Erlebacher J, Aziz MJ, Karma A, Dimitrov N, Sieradzki K (2001) Evolution of Nanoporosity in Dealloying. *Nature* 410: 450-453
12. Tulumieri DJ, Yoon J, Chan MHW (1999) Ordering of Helium Mixtures in Porous Gold. *Phys Rev Lett* 82: 121-124
13. Cortie MB, Maarroof AI, Stokes N, Mortari A (2007) Mesoporous Gold Sponge. *Aust J Chem* 60: 524-527
14. Hayes JR, Hodge AM, Biener J, Hamza AV, Sieradzki K (2006) Monolithic Nanoporous Copper by Dealloying Mn-Cu. *J Mater Res* 21: 2611-2616
15. Pugh DV, Dursun A, Corcoran SG (2003) Formation of Nanoporous Platinum by Selective Dissolution of Cu from Cu<sub>0.75</sub>Pt<sub>0.25</sub>. *J Mater Res* 18: 216-221
16. Zhu JZ, Seker E, Bart-Smith H, Begley MR, Kelly RG, Zangari G, Lye WK, Reed ML (2006) Mitigation of Tensile Failure in Released Nanoporous Metal Microstructures Via Thermal Treatment. *Appl Phys Lett* 89: 133104
17. Dixon MC, Daniel TA, Hieda M, Smilgies DM, Chan MHW, Allara DL (2007) Preparation, Structure, and Optical Properties of Nanoporous Gold Thin Films. *Langmuir* 23: 2414-2422
18. Li R, Sieradzki K (1992) Ductile-Brittle Transition in Random Porous Au. *Phys Rev Lett* 68: 1168-1171
19. Kucheyev SO, Hayes JR, Biener J, Huser T, Talley CE, Hamza AV (2006) Surface-Enhanced Raman Scattering on Nanoporous Au. *Appl Phys Lett* 89: 053102
20. Qian LH, Chen MW (2007) Ultrafine Nanoporous Gold by Low-Temperature Dealloying and Kinetics of Nanopore Formation. *Appl Phys Lett* 91: 083105
21. Hodge AM, Biener J, Hayes JR, Bythrow PM, Volkert CA, Hamza AV (2007) Scaling Equation for Yield Strength of Nanoporous Open-Cell Foams. *Acta Mater* 55: 1343-1349
22. Ding Y, Erlebacher J (2003) Nanoporous Metals with Controlled Multimodal Pore Size Distribution. *Journal of the American Chemical Society* 125: 7772-7773

23. Nyce GW, Hayes JR, Hamza AV, Satcher JH (2007) Synthesis and Characterization of Hierarchical Porous Gold Materials. *Chemistry of Materials* 19: 344-346
24. Hayes JR, Nyce GW, Kuntz JD, Satcher JH, Hamza AV (2007) Synthesis of Bi-Modal Nanoporous Cu, Cu<sub>2</sub>O and Cu<sub>2</sub>O Monoliths with Tailored Porosity. *Nanotechnol* 18: 275602
25. Callister WD (2003) *Materials Science and Engineering: An Introduction*. John Wiley & Sons, Inc., New York
26. Motz C, Pippin R (2001) Deformation Behaviour of Closed-Cell Aluminium Foams in Tension. *Acta Mater* 49: 2463-2470
27. Olurin OB, Fleck NA, Ashby MF (2000) Deformation and Fracture of Aluminium Foams. *Mater Sci Eng A* 291: 136-146
28. Andrews EW, Gioux G, Onck P, Gibson LJ (2001) Size Effects in Ductile Cellular Solids. Part II: Experimental Results. *Int J Mech Sci* 43: 701-713
29. Liu Z, Chuah CSL, Scanlon MG (2003) Compressive Elastic Modulus and Its Relationship to the Structure of a Hydrated Starch Foam. *Acta Mater* 51: 365-371
30. Wilsea M, Johnson KL, Ashby MF (1975) Indentation of Foamed Plastics. *Int J Mech Sci* 17: 457-460
31. Toivola Y, Stein A, Cook RF (2004) Depth-Sensing Indentation Response of Ordered Silica Foam. *J Mater Res* 19: 260-271
32. Ramamurty U, Kumaran MC (2004) Mechanical Property Extraction through Conical Indentation of a Closed-Cell Aluminum Foam. *Acta Mater* 52: 181-189
33. Biener J, Hodge AM, Hamza AV, Hsiung LM, Satcher JH (2005) Nanoporous Au: A High Yield Strength Material. *J Appl Phys* 97: 024301
34. Hakamada M, Mabuchi M (2007) Mechanical Strength of Nanoporous Gold Fabricated by Dealloying. *Scripta Mater* 56: 1003-1006
35. Lee D, Wei X, Chen X, Zhao M, Jun SC, Hone J, Herbert EG, Oliver WC, Kysar JW (2007) Microfabrication and Mechanical Properties of Nanoporous Gold at the Nanoscale. *Scripta Mater* 56: 437-440
36. Volkert CA, Lilleodden ET, Kramer D, Weissmuller J (2006) Approaching the Theoretical Strength in Nanoporous Au. *Appl Phys Lett* 89: 061920
37. Biener J, Hodge AM, Hayes JR, Volkert CA, Zepeda-Ruiz LA, Hamza AV, Abraham FF (2006) Size Effects on the Mechanical Behavior of Nanoporous Au. *Nano Letters* 6: 2379-2382
38. Seker E, Gaskins JT, Bart-Smith H, Zhu J, Reed ML, Zangari G, Kelly R, Begley MR (2007) The Effects of Post-Fabrication Annealing on the Mechanical Properties of Freestanding Nanoporous Gold Structures. *Acta Mater* 55: 4593-4602
39. Lee D, Wei XD, Zhao MH, Chen X, Jun SC, Hone J, Kysar JW (2007) Plastic Deformation in Nanoscale Gold Single Crystals and Open-Celled Nanoporous Gold. *Modelling Simul Mater Sci Eng* 15: S181-S192
40. Mathur A, Erlebacher J (2007) Size Dependence of Effective Young's Modulus of Nanoporous Gold. *Appl Phys Lett* 90: 061910

41. Volkert CA, Lilleodden ET (2006) Size Effects in the Deformation of Sub-Micron Au Columns. *Philos Mag* 86: 5567-5579
42. Davis JR (1998) *Metals Handbook*, ASM International, Materials Park
43. Yamada Y, Wen C, Shimojima K, Mabuchi M, Nakamura M, Asahina T, Aizawa T, Higashi K (2000) Effects of Cell Geometry on the Compressive Properties of Nickel Foams. *Materials Transactions, JIM* 41: 1136-1138
44. Nieh TG, Higashi K, Wadsworth J (2000) Effect of Cell Morphology on the Compressive Properties of Open-Cell Aluminum Foams. *Mater Sci Eng A* 283: 105-110
45. Greer JR, Oliver WC, Nix WD (2005) Size Dependence of Mechanical Properties of Gold at the Micron Scale in the Absence of Strain Gradients. *Acta Mater* 53: 1821-1830
46. Greer JR, Nix WD (2005) Size Dependence of Mechanical Properties of Gold at the Sub-Micron Scale. *Appl Phys A: Mater Sci Process* 80: 1625-1629
47. Wu B, Heidelberg A, Boland JJ (2005) Mechanical Properties of Ultrahigh-Strength Gold Nanowires. *Nature Materials* 4: 525-529
48. Koh SJA, Lee HP (2006) Molecular Dynamics Simulation of Size and Strain Rate Dependent Mechanical Response of Fcc Metallic Nanowires. *Nanotechnol* 17: 3451-3467
49. Zepeda-Ruiz LA, Sadigh B, Biener J, Hodge AM, Hamza AV (2007) Mechanical Response of Freestanding Au Nanopillars under Compression. *Appl Phys Lett* 91: 101907
50. Sun Y, Ye J, Shan Z, Minor AM, Balk TJ (2007) The Mechanical Behavior of Nanoporous Gold Thin Films. *Jom* 59: 54-58
51. Hodge AM, Biener J, Hsiung LL, Wang YM, Hamza AV, Satcher Jr. JH (2005) Monolithic Nanocrystalline Au Fabricated by the Compaction of Nanoscale Foam. *J Mater Res* 20: 554-557
52. Tanimoto H, Fujita H, Mizubayashi H, Sasaki Y, Kita E, Okuda S (1996) Afm Observation of Nanocrystalline Au Prepared by a Gas Deposition Method. *Mater Sci Eng A* 217: 108-111
53. Diao JK, Gall K, Dunn ML (2004) Atomistic Simulation of the Structure and Elastic Properties of Gold Nanowires. *J Mech Phys Sol* 52: 1935-1962
54. Zhou LG, Huang HC (2004) Are Surfaces Elastically Softer or Stiffer? *Appl Phys Lett* 84: 1940-1942
55. Senior NA, Newman RC (2006) Synthesis of Tough Nanoporous Metals by Controlled Electrolytic Dealloying. *Nanotechnol* 17: 2311-2316
56. Doucette R, Biener M, Biener J, Cervantes O, Hamza AV, Hodge AM (2008) Ag Effects on the Elastic Modulus Values of Nanoporous Au Foams *Scripta Mater* to be submitted:
57. Wu HA (2006) Molecular Dynamics Study on Mechanics of Metal Nanowire. *Mech Res Commu* 33: 9-16
58. Biener J, Hodge AM, Hamza AV (2005) Microscopic Failure Behavior of Nanoporous Gold. *Appl Phys Lett* 87: 121908
59. Friedersdorf F, Sieradzki K (1996) Film-Induced Brittle Intergranular Cracking of Silver-Gold Alloys. *Corrosion* 52: 331-336

60. Sieradzki K, Newman RC (1985) Brittle Behavior of Ductile Metals During Stress-Corrosion Cracking. *Phil Mag A* 51: 95-132
61. Kelly RG, Frost AJ, Shahrabi T, Newman RC (1991) Brittle-Fracture of an Au/Ag Alloy Induced by a Surface-Film. *Metall Trans A* 22: 531-541
62. Meinel K, Klaua M, Bethge H (1988) Segregation and Sputter Effects on Perfectly Smooth (111) and (100) Surfaces of Au-Ag Alloys Studied by Aes. *Phys Stat Sol A* 106: 133-144
63. Celarie F, Prades S, Bonamy D, Ferrero L, Bouchaud E, Guillot C, Marliere C (2003) Glass Breaks Like Metal, but at the Nanometer Scale. *Phys Rev Lett* 90: 075504
64. Duxbury PM, Leath PL, Beale PD (1987) Breakdown Properties of Quenched Random-Systems - the Random-Fuse Network. *Phys Rev B* 36: 367-380
65. Kahng B, Batrouni GG, Redner S, de Arcangelis L, Herrmann HJ (1988) Electrical Breakdown in a Fuse Network with Random, Continuously Distributed Breaking Strengths. *Phys Rev B* 37: 7625-7637